Dyeing Uric Acid Crystals with Methylene Blue

Ryan E. Sours, Dorothy A. Fink, and Jennifer A. Swift*

*Department of Chemistry, Georgetown University, 37th and "O" Streets N.W., Washington, DC 20057-1227*

Received March 4, 2002

Abstract: The growth of anhydrous uric acid (**UA**) and uric acid dihydrate (**UAD**) crystals from supersaturated aqueous solutions containing methylene blue, a cationic organic dye, has been investigated. Low concentrations of dye molecules were found to be included in both types of crystal matrixes during the growth process. Incorporation of dye into **UA** crystals occurs with high specificity, affecting primarily {001} and {201} growth sectors, while **UAD** crystals grown from solutions of similar dye concentration show inclusion but little specificity. The orientation of the **UA**-trapped species was determined from polarization data obtained from visible light microspectrometry. To achieve charge neutrality, a second anionic species must also be included with the methylene blue into **UA** and **UAD** crystal matrices. Under high pH conditions, crystallization of 1:1 stoichiometric mixtures of methylene blue and urate yields methylene blue hexahydrate (**MBU·6H₂O**). The crystal structure of **MBU·6H₂O** reveals continuous $\pi-\pi$ stacks of planes of dye cations and urate anions mediated by water molecules. This structure provides an optimal geometry for methylene blue–urate pairs and additional support for the incorporation of these dimers in uric acid single-crystal matrices. The strikingly different inclusion patterns in **UA** and **UAD** demonstrate that subtle changes in the crystal surfaces and/or growth dynamics can greatly affect recognition events.

Introduction

A number of biomineralization studies have examined the processes by which organic molecules are incorporated into crystalline host lattices during growth. The vast majority of these have focused on inorganic crystals (e.g. calcium carbonate, calcium phosphate, and calcium oxalate) which play important assorted roles in nature, such as endo- and exoskeleton formation and calcium storage.[1,2] A handful of organic crystalline materials are equally important constituents of biodeposits, but these have received relatively less attention to date. Crystalline uric acid is a well-established component of some human kidney stones. The crystallization of sodium urate, the ionized form of uric acid, is also the principal clinical symptom of the joint disease gout.[3–5] The causes for uric acid crystallization in vivo are unclear, though several factors including the increased consumption of foods rich in proteins and nucleic acids (e.g. meats),[6] increased cell turnover rates (e.g. during chemotherapy),[7] and other metabolic uric acid regulation problems can lead to elevated serum uric acid concentrations and subsequent precipitation.

The solubility of pure uric acid in aqueous solution depends on solution conditions, particularly pH, ionic strength, and sodium concentration. It is virtually insoluble in all organic solvents and only slightly soluble in water, although its solubility increases with pH. Uric acid exists primarily in its neutral form at low pH; however, above its pK_a of 5.4 the nitrogen at position 3 becomes deprotonated[8] and the major species in solution is urate ion. This pH dependence is an important factor in the kidneys and all along the renal tract, where fluid is gradually acidified and concentrated as water is reabsorbed, hence the proportion of uric acid rises at the same time its solubility rapidly decreases.[9] Abnormally high initial uric acid concentration and/or low urine pH increases the likelihood of uric acid crystal precipitation.
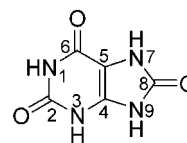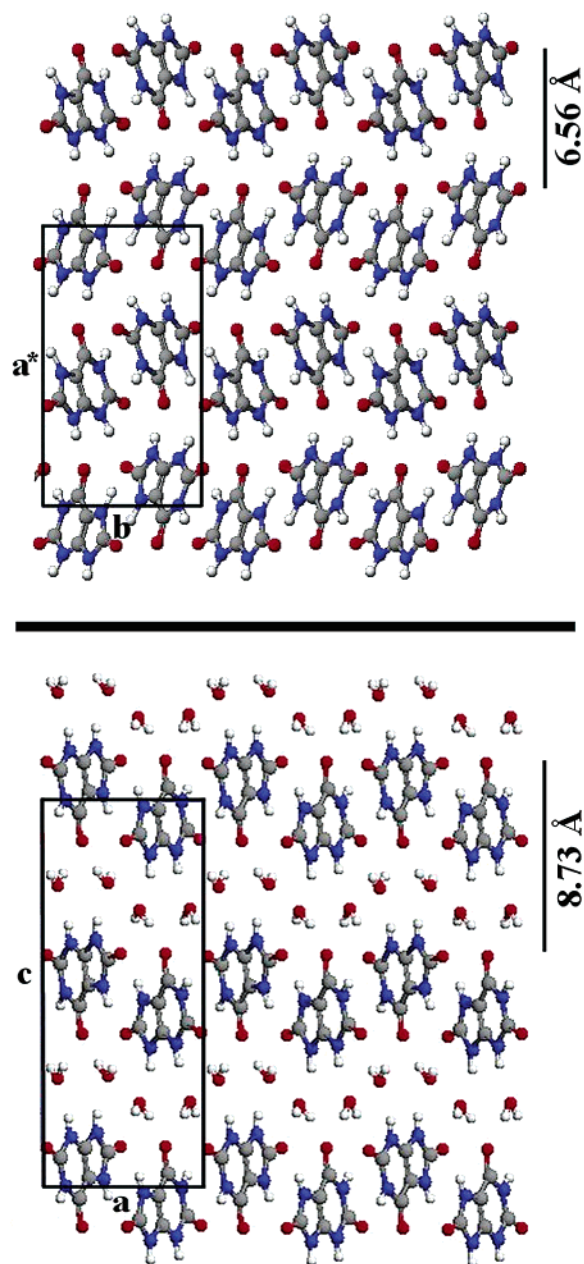

Uric Acid

Supersaturated solutions of uric acid under low pH conditions crystallize to yield either neutral uric acid (**UA**) or uric acid dihydrate (**UAD**) single crystals. Both crystalline phases have been found in human deposits, either alone or often in association with calcium oxalate.[10] It is also not uncommon to find **UA** and **UAD** forms together, as it is known that each

* To whom correspondence should be addressed. E-mail: jas2@georgetown.edu.

(1) Simkiss, K.; Wilbur, K. M. *Biomineralization*; Academic Press: San Diego, CA, 1989.
(2) Lowenstam, H. A.; Weiner, S. *On Biomineralization*; Oxford University Press: New York, 1989.
(3) Howell, R. R.; Evans, E. D.; Seegmiller, J. E. *Arthritis Rheum.* **1963**, *6*, 97–103.
(4) Perl-Treves, D.; Addadi, L. *Proc. R. Soc. London. Ser. B, Biol. Sci.* **1988**, *235*, 145–159.
(5) Perl-Treves, D.; Addadi, L. *Mol. Cryst. Liq. Cryst.* **1990**, *187*, 1–16.
(6) Coe, F. L.; Moran, E.; Kavalich, A. G. *J. Chronic Diseases* **1976**, *29*, 793–800.
(7) Reiselbach, R. E.; Sorenson, L. B., In *Cancer and the Kidney*; Rieselbach, R. E., Garnick, M. B., Eds.; Lea & Febiger: Philadelphia, PA, 1982; pp 506–508.

(8) Mandel, N. S.; Mandel, G. S. *J. Am. Chem. Soc.* **1976**, *98*, 2319–2323.
(9) Wilcox, W. R.; Khalaf, A.; Weinberger, A.; Kippen, I.; Klinenberg, J. R. *Med. Biol. Eng.* **1972**, *10*, 522–531.

Figure 1. Crystal structures of **UA** (top) and **UAD** (bottom), constructed from fractional coordinates.[12,14]

temperature from naturally derived crystals.[13] Another assigns the crystal to the monoclinic space group $P2_1/c$ with $a = 7.237(3)$ Å, $b = 6.363(4)$ Å, $c = 17.449(11)$ Å, and $\beta = 90.51(1)°$, based upon data collected at 120 K from laboratory-grown crystals.[14] In both reports, the **UAD** crystals are highly disordered and/or twinned, which complicated structure refinement. However, a close side-by-side examination of monoclinic and orthorhombic **UAD** structures shows their general crystal packing motifs to be nearly identical. Both structures are very similar to that of **UA,** with the addition of a hydrogen-bonded water layer between adjacent uric acid layers.

Synthetic crystals of **UA** deposit as clear rectangular plates, with large (100) faces bounded by (210), (201), (001), and sometimes (121).[15] **UAD** also crystallizes as clear rectangular plates, with large (001) faces bounded by (011) and (102) and infrequently (210) faces (according to the monoclinic cell convention).[11] While laboratory-grown uric acid crystals are colorless and have well-defined shapes, those formed in vivo are invariably colored and adopt different habits. This indicates the inclusion of impurities, which affects the relative growth rates and colors the crystals.

The observed differences in color and habit between synthetic and natural uric acid crystals prompted us and others[16−21] to examine uric acid crystal growth in the presence of molecular dyes. Gaubert in the 1930s was the first to report that natural and synthetic dyes "stain" laboratory-grown crystals of uric acid. Among the dyes studied was methylene blue, which was reported to include in the crystal matrix without altering the overall crystal morphology. However, his account does not mention whether inclusion in the crystal occurred with any specificity or provide any explanation for the molecular basis for the interaction. Forty years later, Kleeberg revisited the phenomenon of staining uric acid crystals with methylene blue, though his experimental accounts also provide limited information on the specifics of the dye inclusion process or even which uric acid crystal phase was being investigated.
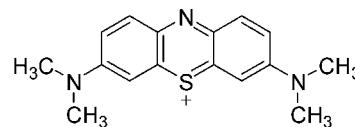
Methylene Blue

We were interested in studying the molecular-level mechanisms by which **UA** and **UAD** crystals grow. Equipped with more advanced analytical techniques and known crystal structures, we embarked on a series of experiments that were initially intended to reproduce earlier work with dyed uric acid crystals, in the hopes that the molecular recognition processes that govern dye inclusion could be elucidated. Organic dyes are ideal preliminary probes for surface recognition because their color

serves as an epitaxial growth substrate for the other.[11] Crystals of **UA** are monoclinic, with a space group of $P2_1/a$ and unit cell dimensions $a = 14.464(3)$ Å, $b = 7.403(2)$ Å, $c = 6.208(1)$ Å, and $\beta = 65.10(5)°$.[12] **UA** adopts a layered motif, with adjacent layers spaced 6.56 Å apart along a^*. Each layer consists of parallel ribbons of uric acid molecules hydrogen bonded head-to-head and tail-to-tail, with the ribbon plane perpendicular to the $b−c$ plane. There is no hydrogen bonding between ribbons within a layer, although ribbons in adjacent layers are hydrogen bonded and offset by ∼62° (see Figure 1).

The structure of uric acid dihydrate has been the subject of some controversy. One report assigns the crystal to the ortho-rhombic space group *Pnab*, based upon data collected at room

(10) Coe, F. L. *Kidney Intl.* **1983**, *24*, 392−403.
(11) Boistelle, R.; Rinaudo, C. *J. Cryst. Growth* **1981**, *53*, 1−9.
(12) Ringertz, H. *Acta Crystallogr.* **1966**, *20*, 397−403.

(13) Artioli, G.; Maschiocchi, N.; Galli, E. *Acta Crystallogr. B* **1997**, *53*, 498−503.
(14) Parkin, S.; Hope, H. *Acta Crystallogr. B* **1998**, *54*, 339−344.
(15) Rinaudo, C.; Boistelle, R. *J. Cryst. Growth* **1980**, *49*, 569−579.
(16) Gaubert, P. *Comptes Rendus* **1936**, *202*, 1192−1194.
(17) Kleeberg, J. *Z. Urol.* **1972**, *8*, 619−629.
(18) Kleeberg, J.; Warski, E.; Shalitin, J. *Adv. Exptl. Med. Biol.* **1974**, *41B*, 821−833.
(19) Kleeberg, J. *Lab. Pract.* **1975**, *24*, 87−88.
(20) Kleeberg, J. *Isr. J. Med. Sci.* **1976**, *12*, 73−76.
(21) Kleeberg, J.; Gordon, T.; Kedar, S.; Dobler, M. *Urol. Res.* **1981**, *9*, 259−261.

is readily apparent when included in the otherwise colorless uric acid crystal matrix. A recent comprehensive review by Kahr and Gurney[22] highlights more than a century of research on a multitude of organic and inorganic dye inclusion crystals. This piece of scholarship was instrumental in bringing our attention to this interesting area of inquiry.
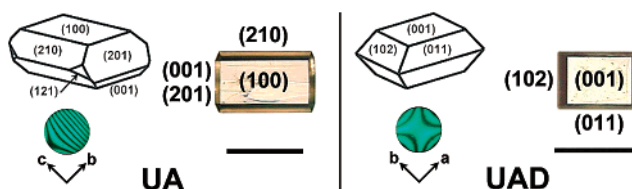
Experimental Section

Crystal Growth. All chemicals were used as received. Water was purified by passage through two Barnstead deionizing cartridges followed by distillation. Supersaturated solutions were prepared by dissolving 15−20 mg of uric acid (Aldrich, 99+%) in 100 mL of boiling deionized water. Pure small (200−300 μm) single crystals of uric acid dihydrate (**UAD**) and uric acid (**UA**) grew upon standing at room temperature (24 ± 1 °C) and in a water bath (37 ± 0.1 °C), respectively. While pH is important in uric acid crystal growth, solutions prepared with the above temperature and concentration combinations were of pH 4−5 and no further pH adjustment was made.

A stock dye solution was prepared by dissolving 50 mg of methylene blue (C.I. 52015) (Aldrich, 98%) in 100 mL of deionized water. Dye solution was added to the supersaturated uric acid solutions to yield a final dye concentration of 2−100 μM (~10−600:1 uric acid−methylene blue). The resulting blue solution was cooled and allowed to crystallize at 24 or 37 °C. After 1−7 days, small (200−300 μm) plate-shaped single crystals with blue dye inclusions (**UA-MB** and **UAD-MB**) were transferred to a glass microscope slide with a disposable Pasteur pipet, and examined with polarized optical microscopy and microspectrophotometry.

Dye Concentrations in UA-MB and UAD-MB. Methylene blue is difficult to quantify by absorption spectroscopy because of its tendency to dimerize in solution, resulting in a shoulder on the low-wavelength side of the monomer peak.[23] Two calibration plots (one for the absorbance at 662 nm and the other for the integrated absorbance) were made for methylene blue concentrations between 6.5 and 260 μM in the presence of 8 mM uric acid at pH 10. Several milligrams of either **UA-MB** or **UAD-MB** was dissolved in water at pH 10, and the absorbance at 662 nm and integrated absorbance were compared to the calibration curves. Standard addition was also performed and the resulting concentrations were in agreement with those from the calibration curves.

Cocrystals of Methylene Blue and Urate. A supersaturated urate solution was prepared by dissolving 100 mg of uric acid in 100 mL of boiling 0.05 M aqueous phosphate buffer, for a final solution of pH 6.4 (24 °C). Methylene blue (MB) was added in a 1:1 molar ratio with uric acid to make an opaque deep blue solution. After several days at either 24 or 37 °C, gold metallic thin plates and/or block-shaped crystals of methylene blue urate hexahydrate (**MBU·6H$_2$O**) were deposited from these standing supersaturated aqueous solutions.

X-ray Crystallography. The structure of **MBU·6H$_2$O** was solved by single-crystal X-ray diffraction. **MBU·6H$_2$O** crystals are triclinic with space group $P\bar{1}$, $Z = 2$ and cell parameters $a = 10.285(2)$ Å, $b = 11.387(2)$ Å, $c = 11.606(2)$ Å, $\alpha = 83.273(3)°$, $\beta = 78.792(3)°$, and $\gamma = 76.547(3)°$. The final R_1 ($I > 2\sigma$) was 0.0613. Data were collected (full Ewald sphere) on a Siemens SMART Platform CCD diffractometer with graphite monochromated Mo Kα radiation ($\lambda = 0.71073$) at 173 K. The structure was solved by direct methods (SHELXTL, V5.0, Siemens Industrial Automation, Inc., Madison, WI) and refined by using full-matrix least-squares/difference Fourier techniques. The occupancy of the disordered urate molecule was refined in two different positions (occupancies of 0.63 and 0.37) related by slight translation down the long axis of the molecule. With a urate in the minor occupied position, a seventh water molecule per asymmetric unit was introduced and refined with an identical occupancy. All non-hydrogen atoms (with

(22) Kahr, B.; Gurney, R. W. *Chem. Rev.* **2001**, *101*, 893−952.
(23) Rabinowitch, E.; Epstein, L. F. *J. Am. Chem. Soc.* **1941**, *63*, 69−78.

Figure 2. Schematic, micrograph, and conoscopic interference pattern (at 505 nm) of synthetic **UA** (left) and **UAD** (right) single crystals. Miller indices for **UAD** are based on monoclinic cell conventions. Scale bars = 250 μm.

the exception of the oxygen atom in the seventh water molecule) were refined with anisotropic displacement parameters. Some hydrogen atoms were found in difference maps while others were introduced in idealized positions, but all were refined isotropically. Due to the disorder, some of the hydrogen atoms could not be located. The absorption correction was applied with the Siemens Area Detector ABSorption program (SADABS).

Visible Microspectrophotometry. Visible absorption spectroscopy of dye-inclusion crystals was achieved by using a modified Olympus BX50 polarizing microscope. An Ocean Optics PC2000-ISA spectrometer optimized for the visible region was coupled via a 2 m × 600 μm diameter fiber optic patch cable (P600-2UV/Vis) to a home-built adapter inserted into a Diagnostic Instruments DBX phototube on the microscope. This arrangement allowed absorption measurements using a 50× UMPlanFl objective in convergent light on a spot size approximately 10−15 μm in diameter. Spectral acquisition was accomplished with Ocean Optics OOIBase32 software and Microsoft Excel 2000 was used for data analysis. The PC2000-ISA is configured with a grating (no. 3) with 600 lines/mm blazed at 500 nm, OFLV-3 coated, 2048 element, linear CCD detector with L2 collection lens, and a 10 μm slit. The bandwidth is limited to 400−750 nm by the microscope optics and lamp, with an overall spectral resolution of 1.02 nm fwhm.

Results and Discussion

Pure Synthetic Crystals. Pure synthetic crystals of either **UA** or **UAD** were grown in the laboratory by controlling temperature and supersaturation.[15] We found that **UA** growth is generally favored from high-temperature (37 °C) and low-supersaturation solution conditions. The growth of **UAD** crystals is favored from conditions promoting faster growth, such as lower temperature (24 °C) and higher supersaturation levels. Crystals of **UAD** are less stable and slowly decompose (by dehydration)[11] to form polycrystalline **UA** in air or solution over a period of hours or days, respectively. Both **UA** and **UAD** crystals adopt habits identical with those in previous reports and are typically ~250 μm in their largest dimension (see Figure 2).

Though both materials are clear colorless plates, distinguishing **UA** and **UAD** proved to be relatively straightforward by differences in the FTIR-ATR spectra (**UAD** shows a strong water absorption band at ~3400 cm^{-1}) or conoscopic light interference patterns. **UA** and **UAD** crystals are biaxial positive and negative, respectively.[24] The optic plane for **UA** is tilted 45.6° from the large (100) plate face,[25] whereas the optic plane for **UAD** is perpendicular to the large (001) plate face. Conoscopic interference patterns are sometimes difficult to see with polychromatic light, but with a 505 nm interference filter, the differences are unambiguous. This method proved to be the easiest for rapidly identifying **UA** and **UAD** phases and crystallographic directions in each.

(24) Ringertz, H. *Acta Crystallogr.* **1965**, *19*, 286−287.
(25) Shirley, R. *Science* **1966**, *152*, 1512−1513.
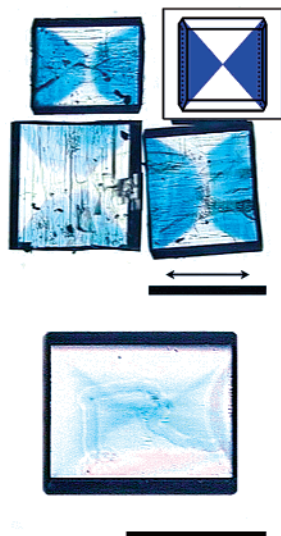
Figure 3. Polarized photomicrograph of **UA-MB** inclusion crystals (top) with idealized representation of a **UA-MB** crystal showing dye inclusion in {001} and {201} growth sectors (inset). Scale bar = 250 μm. Polarized photomicrograph of a **UAD-MB** inclusion crystal (bottom). Scale bar = 100 μm. The arrow indicates incident polarization direction.

Dye Inclusion Crystals. Dyes are excellent probes for crystal growth studies because inclusion of even small amounts in a crystalline host matrix can be detected. We grew crystals of uric acid from supersaturated aqueous solutions containing methylene blue concentrations ranging from 2 to 100 μM. Crystals obtained at 37 °C, **UA-MB**, showed hourglass patterns of color resulting from dye inclusion in {001} and {201} growth sectors (see Figure 3). When viewed under linearly polarized light, sectors containing dye appear significantly more intense when the incident polarization is parallel to the *c* axis of the crystal (*c* is used in place of *c** due to the pseudo-orthorhombic packing). This suggests that the methylene blue molecules included in these sectors are preferentially oriented. Interestingly, the dye-included crystals showed no obvious change in their macroscopic habit or relative size compared to unstained **UA** crystals.

Average dye concentrations were determined by dissolving several **UA-MB** crystals in water at high pH and measuring the visible absorbance. From these measurements, we estimate that **UA-MB** crystals contain between 2 and 12 dye molecules per 10^4 molecules of uric acid, depending on the initial solution dye concentration. This concentration is comparable to that reported for other dye inclusion crystal systems.[26,27] In all cases, only a small fraction (<1%) of the free methylene blue in solution is actually included in the **UA** matrix during growth.

UAD crystals grown from solutions containing similar solution methylene blue concentrations yielded very different results. Dye inclusion in **UAD-MB** does not, in general, appear specific for particular growth sectors, although at the highest dye concentrations some selectivity for {210} appears to be a possibility (see Figure 3). The dihydrate crystals have a much paler color than their anhydrous counterparts. When viewed under linearly polarized light, the blue pattern is most intense

when the incident polarization is parallel to the *b* axis of the crystal. This suggests that the methylene blue molecules included in the crystal may be preferentially oriented, even though they lack selectivity for specific growth sectors. Again, the dye-included crystals showed no change in their macroscopic habit or relative size compared to unstained **UAD** crystals. **UAD-MB** crystals contain between 3 and 30 dye molecules per 10^4 molecules of uric acid—approximately twice the amount included in **UA-MB**. This apparent discrepancy may be attributed to the selectivity difference between the two forms. Dye is included throughout the **UAD-MB** crystal, whereas it is confined to the {001} and {201} sectors in **UA-MB**.

Linear Dichroism. Methylene blue has C_{2v} symmetry, with the 2-fold axis passing through the central ring nitrogen and sulfur atoms. The transition dipole for the visible absorption lies along the long axis of the molecule, perpendicular to the 2-fold axis.[28,29] Linear dichroism measurements on **UA-MB** and **UAD-MB** single crystals were made with a home-built micro-spectrophotometer, constructed by interfacing an Ocean Optics PC visible spectrometer to a polarizing microscope. Absorption intensities between 400 and 750 nm could be obtained on crystal areas as small as $10-15$ μm in diameter by using the highest power objective (50×). These dimensions were well-suited for dyed uric acid crystals, which typically reach only ~30 μm in their smallest dimension.

Absorption spectra were collected at two orthogonal polarization directions for each of three orthogonal viewing directions (see Figure 4). Integrated intensities were calculated from a best fit of three Gaussians to baseline-corrected absorption spectra. The spectra for both polarizations along *b* in **UA-MB** showed an overlying low-frequency oscillation most likely due to substantial elliptical/circular polarization caused by the crystal. Since **UA** is monoclinic, with $\beta = 65.10°$, the *a** direction is normal to the large (100) plate face. However, the *b* and *c* directions do not look down on low index faces. Similarly, for **UAD-MB** the *c* axis is perpendicular to the large (001) plate face but faces perpendicular to the *a* and *b* axes are not present. The small size and brittleness of the crystals defeated attempts to cut and polish faces perpendicular to the *b* and *c* (**UA**) or *a* and *b* (**UAD**) axes, so measurements in those directions were made on the naturally angled faces. No attempt was made to correct the observed spectra for reflection losses from the crystal surfaces.

Since the birefringence is relatively high for **UA** and **UAD** ($B = 0.31$ and 0.22), the contribution of the anisotropic crystal matrix to the local electric field around the included dye molecules could not be ignored.[30] Several methods of varying rigor are available to correct measured absorption intensities for matrix refractive index differences.[31] The dichroic ratio, *N*, is determined by taking the ratio of the two orthogonal integrated intensities, *D*, for each viewing direction. The corrected dichroic ratio, *N**, is given by $g \cdot N$, where g is a correction factor calculated from the refractive indices. We chose to use the method of Vuks,[32] which ignores the birefringence and assumes an isotropic local field with $\langle n^2 \rangle = (n_\alpha^2 + n_\beta^2 + n_\gamma^2)/3$. The

(26) Mitchell, C. A.; Lovell, S.; Thomas, K.; Savickas, P.; Kahr, B. *Angew. Chem., Intl. Ed. Engl.* **1996**, *35*, 1021−1023.
(27) Lovell, S.; Subramony, P.; Kahr, B. *J. Am. Chem. Soc.* **1999**, *121*, 7020−7025.
(28) Bergmann, K.; O'Konski, C. T. *J. Phys. Chem.* **1963**, *67*, 2169−2177.
(29) Campbell, D. J.; Higgins, D. A.; Corn, R. M. *J. Phys. Chem.* **1990**, *94*, 3681−3689.
(30) Michl, J.; Thulstrup, E. W. *Spectroscopy with Polarized Light*; VCH Publishers: New York, 1986.
(31) Blinov, L. M. *Electro-Optical and Magneto-Optical Properties of Liquid Crystals*; John Wiley & Sons Limited: Chichester, UK, 1983.
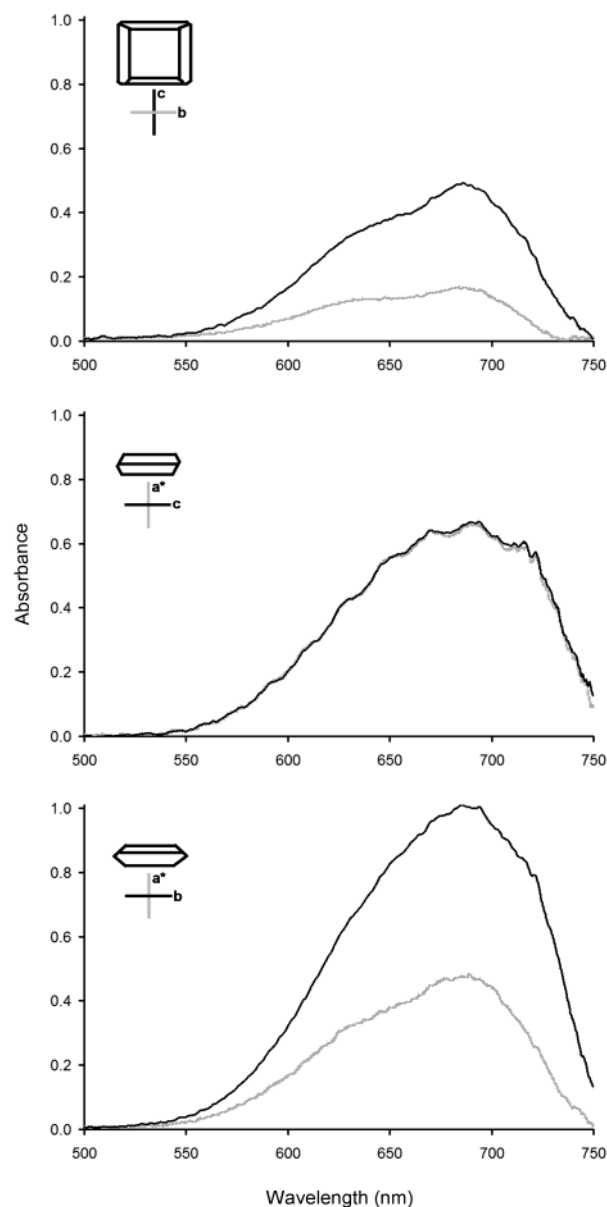
Figure 4. Baseline-corrected absorption spectra for **UA-MB** crystals with polarized light incident along the a^* axis (top), the b axis (middle), and the c axis (bottom). Labeled axes below crystal figures indicate the orientation of the incident polarization with respect to the crystal.

Vuks method is reported to work well experimentally for anisotropic crystals, and is a compromise between the experimentally less valid Lorentz model and the extremely rigorous Dunmur method.[33,34] The resulting correction factor is the ratio of the refractive indices orthogonal to the viewing direction, and the corrected dichroic ratio is given by

$$N^* = \frac{n_1 D_1}{n_2 D_2} \tag{1}$$

For monoclinic crystals, the refractive indices do not all necessarily lie along crystallographic directions. This is true for **UA**, in which n_α (1.588) lies along b, while n_β (1.739) and n_γ (1.898) are offset by 45.6° from a^* and c.[24,25] Therefore, the average of n_β and n_γ was used for the refractive index along a^*

(32) Vuks, M. F. *Opt. Spectrosc.* **1966**, *20*, 361–364.
(33) Dunmur, D. A. *Chem. Phys. Lett.* **1971**, *10*, 49–51.
(34) Dunmur, D. A. *Mol. Phys.* **1972**, *23*, 109–115.

Table 1. Linear Dichroism Data for **UA-MB** and **UAD-MB**

	ratio[a]	g	N	N*	θ[b]
UA-MB	a^* (b/c)	0.873	0.311	0.272	27.5
	b (a*/c)	1.000	0.984	0.984	44.8
	c (a*/b)	1.145	0.431	0.493	35.1
UAD-MB	a (b/c)	0.979	0.945	0.925	43.9
	b (a/c)	0.873	0.752	0.656	39.0
	c (a/b)	0.892	0.446	0.446	33.7

[a] Given as viewing direction (polarization direction ratio). [b] Dipole direction, measured in degrees from the upper polarization direction in ratio.

and c. For **UAD**, n_α (1.508) lies along a and n_β (1.691) along b, with n_γ (1.728) along c. When calculating N^*, we assumed that the refractive indices were constant for the wavelength region 500–750 nm. The visible absorption spectrum for methylene blue is complicated and highly dependent on the surrounding medium. In aqueous solution, the monomer has a maximum at 664 nm that shifts to 746 nm in strongly acidic conditions, while the dimer spectrum has peaks at 605 and 685 nm.[35] The shorter wavelength peak (P-band) is due to the face-to-face sandwich-type dimer and the higher wavelength peak (N-band) is the result of end-to-end dimerization.[36] In solution, the P-band dominates the dimer spectrum. The absorption maximum for crystals of pure methylene blue is 578 nm.[37] When included in Nafion film, absorption bands are observed at 650 (monomer), 590 (dimer), and 745 nm (protonated monomer).[38] Dyes trapped in organic crystal matrices typically exhibit a red-shift in their visible absorption spectra. For example, inclusions of methylene blue in meconic acid have an absorption maximum at 680 nm, a red-shift of 16 nm from the solution maximum.[27] We found that the absorption maximum for methylene blue in **UA-MB** was nearly constant at 688 nm, regardless of polarization. However, the absorption peak for **UAD-MB** was highly dependent on the incident polarization direction and varied from 650 to 708 nm. The variation in peak wavelength observed for **UAD-MB** for different polarization directions may indicate multiple populations (different orientations in distinct environments or aggregates). Electronic spectroscopy inherently averages orientational sub-populations, and can give rise to false calculated orientations. Therefore, methylene blue orientation in **UAD** matrices may not be as reliable as that in **UA-MB**.

Dye Orientation. The methylene blue transition dipole calculated from the above linear dichroism results was incorporated into the **UA** and **UAD** cells (see Figure 5 and the Supporting Information). The alignment of the calculated dipole coincides with the ribbon directions in both the **UA** and **UAD** crystal structures. The absolute direction of the polar axis is not easily determined, but based on the dipole direction and surrounding crystal structure, we assumed a face-to-face stacking interaction between uric acid and methylene blue[39] molecules in each crystal lattice (see Figure 5). This limits rotational orientation about the dye's long axis to two possibilities. The translational position of the dye within the crystal matrix was inferred such that the dye is confined to a single uric acid layer, based on steric considerations. The dye has an available hydrogen bond acceptor, and it seems reasonable to satisfy this

(35) Nishikiori, H.; Nagaya, S.; Tanaka, N.; Katsuki, A.; Fujii, T. *Bull. Chem. Soc. Jpn.* **1999**, *72*, 915–921.
(36) Patil, K.; Pawar, R.; Talap, P. *Phys. Chem. Chem. Phys.* **2000**, *2*, 4313–4317.
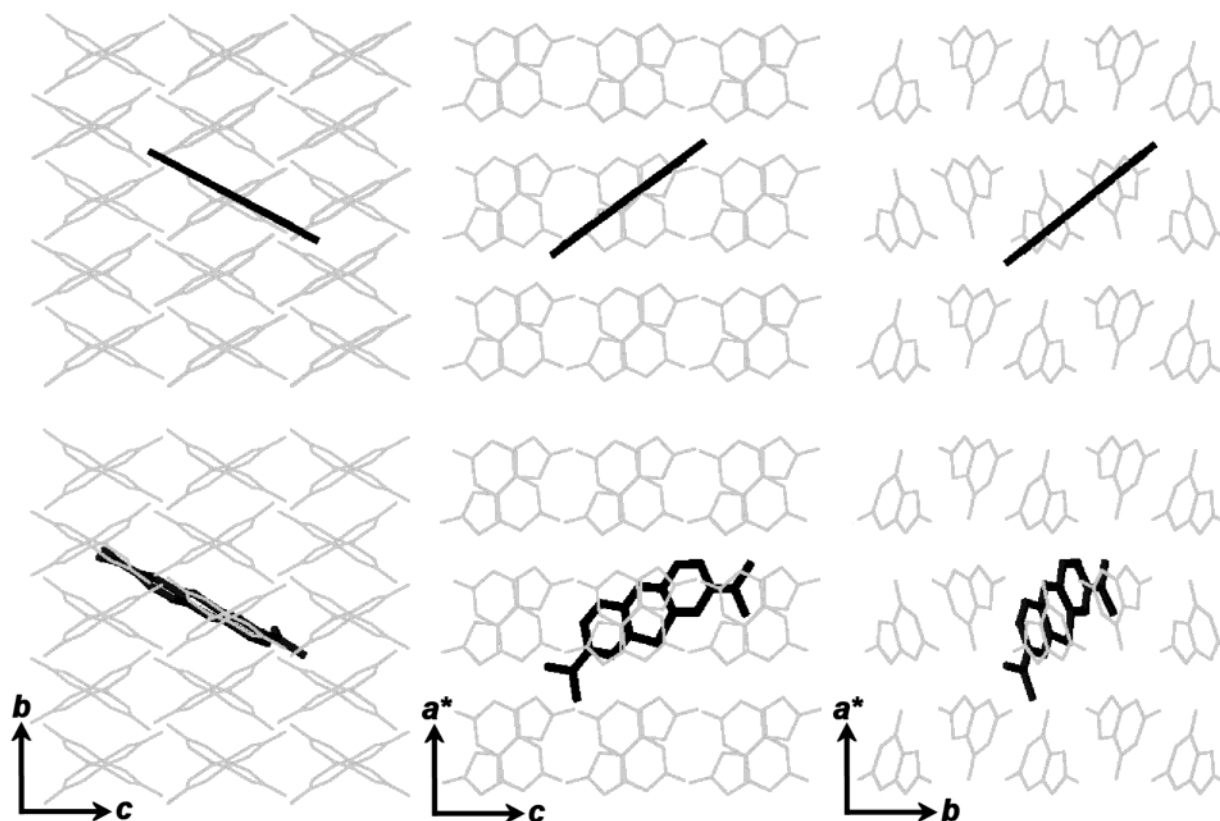(37) Demon, L. *Ann. Phys.* **1946**, *12*, 101–141.
(38) John, S. A.; Ramaraj, R. *Langmuir* **1996**, *12*, 5689–5695.
(39) Marr, H. E. I.; Stewart, J. M.; Chiu, M. *Acta Crystallogr. B* **1973**, *29*, 847–853.

Figure 5. **UA** crystal structure viewed down *a**, *b*, and *c* showing the experimentally determined dipole (top) and possible orientation of the methylene blue molecule (bottom).

site. When the dye is positioned to satisfy hydrogen bonding with the adjacent layer, its ring nitrogen approximately replaces the uric acid carbonyl at C6.

However, this simple picture does not fully explain the inclusion process. In inorganic biomineralization processes, the proteins included during growth typically have anionic side chains,[2] which are believed to be important in regulation of the size and shape of the host matrix. The macromolecular impurities are much larger than the individual components of the host in these systems, and presumably charge balance can be attained by slight adjustment of the number of the host cations/anions. In our dye inclusion crystals, methylene blue cations and neutral uric acid molecules are much more similar in size. It seems unlikely that a neutral host matrix would be able to incorporate large numbers of cations without parallel inclusion of anions for charge balance.

In both **UA-MB** and **UAD-MB** crystallization, the methylene blue dye used was a chloride salt, making chloride the first logical choice of anion incorporated in the crystals. However, we were unable to detect chloride in solutions of dissolved crystals by potentiometry. To more specifically test the influence of chloride ion on the inclusion crystals, we removed chloride ion from solution by acetate ion exchange through precipitation of silver chloride with silver acetate. Uric acid crystals grown in the presence of methylene blue acetate appeared indistinguishable from those grown in the presence of methylene blue chloride. On the basis of steric arguments, it is not obvious how chloride and acetate ions would both occupy similar positions in **UA-MB** and **UAD-MB** crystal lattices.

The other possible anion source in solution was uric acid itself, which even at low pH is partially ionized to urate (~12%

at pH 4.5). We rationalized that the urate geometry would almost certainly permit easy substitution for a uric acid molecule in the **UA** or **UAD** crystal lattice. The red-shifted maximum absorption observed in **UA-MB** at 687 nm (relative to the solution max at 664 nm) is also consistent with shifts previously seen for methylene blue in solution with various organic anions.[40,41] It therefore seemed likely that a 1:1 complex between methylene blue and urate was the most plausible species accounting for the dye inclusion in uric acid hosts. One remaining question was whether the optimal geometry of the methylene blue−urate pairs would support or contradict our proposed methylene blue orientation.

Methylene Blue−Urate Geometry. In most aromatic $\pi-\pi$ systems, molecules typically pack in either face-to-face or edge-to-face geometries. To the best of our knowledge, the geometry of organic cation−urate pairs has not been previously reported. However, molecular dynamics simulation has been used to calculate the conformation of an aqueous methylene blue−guanine complex, which forms face-to-face stacked pairs.[42] Guanine is structurally similar to uric acid, so we anticipated a face-to-face geometry for a methylene blue−urate complex. With this in mind, we sought to investigate the pair geometry directly by growing cocrystals of methylene blue urate. Above pH 5.4, the majority of uric acid exists as urate. Supersaturated solutions of equimolar uric acid and methylene blue chloride at pH = 6.4 yielded metallic gold plate-shaped crystals of methylene blue urate hexahydrate, **MBU·6H₂O**.

(40) Hamai, S. *Bull. Chem. Soc. Jpn.* **1985**, *58*, 2099−2106.
(41) Hamai, S.; Satou, H. *Bull. Chem. Soc. Jpn.* **2000**, *73*, 2207−2214.
(42) Enescu, M.; Levy, B.; Gheorghe, V. *J. Phys. Chem. B* **2000**, *104*, 1073−1077.
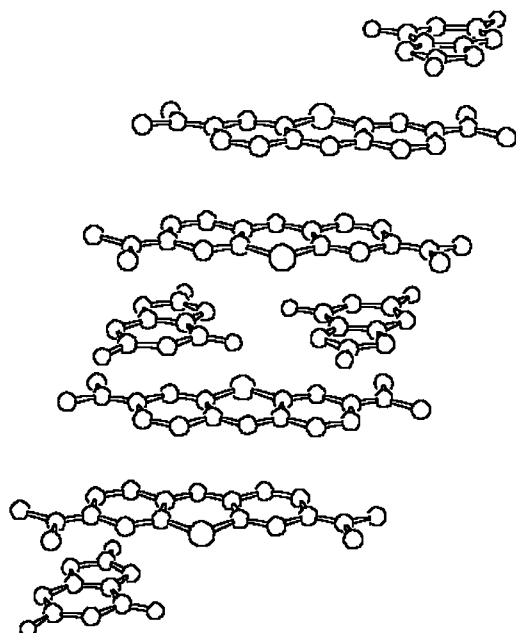
Figure 6. Packing diagram of **MBU·6H₂O** showing $\pi-\pi$ stacking (water molecules and hydrogen atoms omitted for clarity).

MBU·6H₂O crystallizes in a layered structure, with the plane of each molecule parallel to the layers (see Figure 6). Layers are composed of exclusively urate or methylene blue ions, with water molecules interspersed within and between the ionic layers. Methylene blue is approximately twice the size of urate, so that two layers are required for every one urate layer to satisfy charge balance. Negatively charged urate layers are held together by a two-dimensional network of hydrogen bonds mediated by water molecules. Perhaps not surprisingly, the topology of the urate layers is very similar to that in sodium urate monohydrate.[8] Methylene blue molecules within a layer are oriented identically, with the long axis along (011). Adjacent methylene blue layers are related by an inversion center. The interlayer spacing along *a* is 3.43 Å, which is between the reported spacings of 3.28 Å for sodium urate monohydrate[8] and 3.50 Å for methylene blue chloride pentahydrate.[39]

Linear dichroism measurements on **MBU·6H₂O** crystals were not possible due to the optical density of the crystals. However, very thin plates of **MBU·6H₂O** were collected and examined with polarized microscopy. One of the angles on the plate face was measured as 83°, which corresponds to α (83.273°) from the crystal structure. We surmised that the large plate face is (100) and the smaller side faces (010), (001), and sometimes (011). According to the crystal structure, the long axis of each methylene blue molecule lies along [011]. When viewed under transmitted polarized light, the crystal exhibited maximum absorption (opacity) when the polarization direction bisected α (see Figure 7). The visible absorption dipole for methylene blue corresponds to the long axis of the molecule, in agreement with previous calculations.[28,29]

Conclusions

We have demonstrated that the inclusion of methylene blue in uric acid single crystals occurs with far more specificity than previous reports have detailed. The presence of methylene blue in solution during uric acid crystal growth results in oriented inclusion of low concentrations of the dye in the crystal matrix.
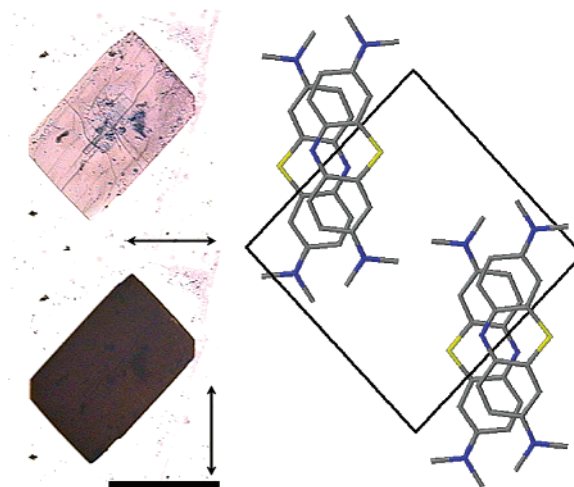
Figure 7. Polarized photomicrographs of a **MBU·6H₂O** crystal at two orthogonal polarization directions (indicated by arrows, left). Scale bar = 100 μm. The orientation of methylene blue in the unit cell, viewed along *a* (right).

In **UA-MB** crystals, dye is localized in the {001} and {201} growth sectors. Little specificity is apparent in the case of **UAD** matrices. The orientation of the included dye molecules was determined from linear dichroism measurements and correlated with the host crystal structure. Methylene blue−urate dimers were rationalized as the most reasonable species included for charge balance. A reasonable geometry for $\pi-\pi$ stacked ion pairs included in **UA** and **UAD** hosts was obtained from the structure of methylene blue urate cocrystals (**MBU·6H₂O**).

Unfortunately, knowledge of the dye orientation does not explain the affinity of the dye for only the {001} and {201} growth sectors of **UA-MB**. The geometry of methylene blue−urate pairs should also be acceptable for inclusion in **UAD-MB** matrices, and at present we can offer no explanation on the basis of chemical interactions for why the inclusion patterns in **UA** and **UAD** are so different. Given the overall rectangular shape of both crystal forms, one might expect the macroscopic growth rates to be similar for the [010] and [001] directions in **UA** and the [100] and [010] directions in **UAD**. Therefore, macroscopic growth rates fail to explain the sectoring. The answer is likely related to subtle differences in growth kinetics and mechanisms on the molecular level, and future work will address this.

Supporting Information Available: Figures similar to Figures 4 (absorption spectra) and 5 (dipole orientation and average dye orientation) for **UAD-MB**; atomic coordinates, bond lengths and angles, and anisotropic displacement parameters; thermal ellipsoid plots; and structural diagrams for **MBU·6H₂O** (PDF). This material is available free of charge via the Internet at http://pubs.acs.org.

JA026083W